

Cite this: *Catal. Sci. Technol.*, 2019, 9, 6327

Manganese PNP-pincer catalyzed isomerization of allylic/homo-allylic alcohols to ketones – activity, selectivity, efficiency†

Tian Xia, ‡ Brian Spiegelberg, ‡ Zhihong Wei, ‡ Haijun Jiao, Sergey Tin, Sandra Hinze and Johannes G. de Vries *

Received 27th July 2019,
Accepted 10th October 2019

DOI: 10.1039/c9cy01502g

rsc.li/catalysis

We report the first manganese catalyzed isomerization of allylic alcohols to produce the corresponding carbonyl compounds. The ligand plays a decisive role in the efficiency of this reaction. Very high conversions could be obtained using a solvent-free reaction system. A detailed DFT study reveals a self-dehydrogenation/hydrogenation reaction mechanism which was verified by the isolation of the α,β -unsaturated ketone as intermediate and a deuterium labeling experiment. It also provided a rationale for the observed selectivity and the higher efficiency of phenyl over isopropyl substitution.

1. Introduction

Atom economy has been widely used in synthesis and catalysis as an important metric, since Trost proposed this concept in 1995.¹ Alkene isomerization is one of the prime examples of atom economy and green chemistry because all atoms from the substrate are used to form the product without generation of any waste.² One of the most interesting and widely investigated isomerization reactions is the transformation of readily available allylic alcohols into ketones and aldehydes which are the basic components of many chemicals in both laboratory and industry.³ During the last half century, numerous all-around and highly active homogeneous allylic alcohol isomerization catalysts, containing precious transition metals like Ir, Ru, Pd and Rh have been widely investigated.³ However, noble metals are expensive and there are severe limitations on their use in the production of pharmaceuticals, in particular in the last step of a synthetic sequence. Consequently, much attention has been focused on their replacement with first-row transition metals which are earth-abundant, environmentally friendly and often less toxic. Recently, reports have appeared on the sole use of base as catalyst for the isomerization of allylic alcohols to the corresponding ketones.⁴

Homogeneous manganese catalysts were found to be effective catalysts for hydrogenation,⁵ dehydrogenation,⁶ transfer hydrogenation,⁷ alkyne semi-hydrogenation,⁸ CH-activation reactions,⁹ hydrosilylation reactions¹⁰ and

dehydrogenative alkylation reactions.¹¹ Although excellent results in various chemical processes have been obtained by using manganese pincer complexes as catalysts, isomerization reactions of allylic alcohols to produce ketones are still unknown so far. We have previously reported the isomerization of allylic alcohols using iron and cobalt PNP pincer complexes.¹² Herein, we report the first manganese-catalyzed isomerization of allylic/homo-allylic alcohols to ketones.

First, we decided to screen a number of different manganese PNP pincer complexes. The first PNP pincer ligated manganese complex was reported by Nocera and Ozerov in 2009. This complex was prepared by a reaction of the PNP ligand with $Mn_2(CO)_{10}$ or $Mn(CO)_5Br$ to afford $(PNP)Mn(CO)_3$.¹³ This method has been utilized as a model reaction in the syntheses of many other PNP manganese complexes. Subsequently, Boncella and co-worker synthesized and characterized a range of PNP pincer manganese

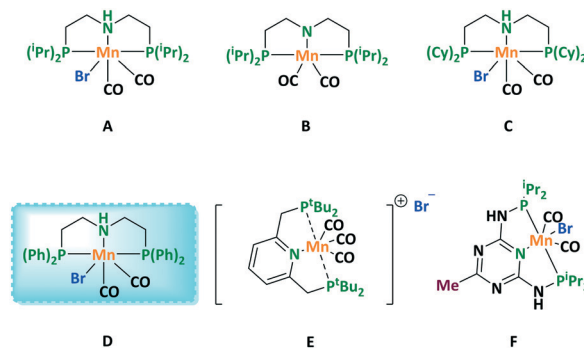


Fig. 1 PNP-Mn complexes A-F tested in the isomerization of allylic alcohols.

Leibniz-Institut für Katalyse e.V. an der Universität Rostock, Albert-Einstein-Strasse 29a, 18059 Rostock, Germany. E-mail: johannes.devries@catalysis.de

† Electronic supplementary information (ESI) available. See DOI: 10.1039/c9cy01502g

‡ These authors contributed equally to this work.

complexes of which complex A (Fig. 1) is an example.¹⁴ In order to investigate the role of substitution on the efficiency of the isomerization we tested the complexes B, C and D hitherto known for hydrogenation, *N*-alkylation and dehydrogenative coupling.^{5a,11aj} Beyond the PNHP ligand sphere we were interested in testing complexes E and F due to their different structural motif and catalytic performance in dehydrogenative coupling and hydrogenation reactions.^{5b,15}

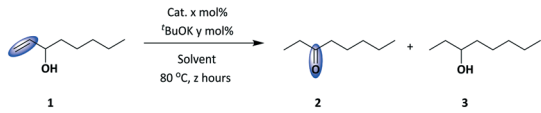
2. Results and discussion

2.1 Screening and optimization of the isomerization

Our initial experiments were performed at 80 or 120 °C in different solvents using oct-1-en-3-ol as substrate in the presence of a catalytic amount of manganese compounds A–F (Table 1, full screening see ESI†). Only 3% of ketone was observed by using toluene as solvent in 20 hours at 80 °C with compound A and ^tBuOK (Table 1, entry 1). Then toluene was replaced by THF and a higher conversion and yield (17%) was obtained (entry 2). By using different solvents in the presence of complex B which presumably is the active catalyst that forms from A in the presence of base, we found heptane was a somewhat better solvent than THF and toluene (entries 3–5). Furthermore, higher conversions and yields were observed by using 5 mol% of compound B in both 1 and 9 hours at 120 °C (entries 6–7). Interestingly, 69% of the desired product was obtained by using neat condition after 9 hours (entry 8). Complex C was used as catalyst in heptane or under neat condition at 120 °C, which resulted in good conversions and yields (entries 9–12). To our delight,

we found that the best results were obtained using D as catalyst, with quantitative conversion at 120 °C in only two hours (entry 13). Relatively poor results were obtained with the Milstein catalyst (E) (entries 14–16) and the Kempe catalyst (F) (entries 17–19). Next, we optimized the reaction conditions of the reaction catalyzed by complex D. Use of 1,4-dioxane, which is a good solvent for ester hydrogenation catalyzed by complex D, resulted in the highest amount (98%) of ketone (Table 2, entry 2). This catalyst showed the same selectivity in both toluene and cyclohexane (entries 1 and 3). Compared to other solvents, the reaction in heptane resulted in poor selectivity under the same reaction conditions (entry 4). Under neat conditions, full conversion of the substrate was observed with 97% yield of the desired product (entry 5). Decreasing catalyst and base loadings to 1 mol% resulted in quantitative conversion and yield of the desired product at 120 °C after 1 hour in 1,4-dioxane (entry 6). Surprisingly, this catalytic reaction also showed good conversion and yield even at room temperature after both 1 hour and 16 hours (entry 7). Furthermore, the conversion and yield dropped when the catalyst and ^tBuOK loadings were decreased to 0.1 mol% in 1,4-dioxane (entry 8). Catalyst D (0.1 mol%) showed high activities in both cyclohexane and toluene (entries 9–11). It is worth mentioning that the isomerization reaction proceeds in neat oct-1-en-3-ol and yields 94% of the desired 3-octanone (entry 12). The catalytic activity of compound D was also tested under the same reaction conditions at room temperature (entry 13). However, this led to a dramatic decline of its activity (6% yield after 16 h). On the other hand, we were interested in finding the maximum efficiency of catalyst D, for which reason we

Table 1 Catalyst screening in oct-1-en-3-ol isomerization^a



Entry	Cat. (%)	^t BuOK (%)	Solvent	Time (h)	Conv. ^b [%]	Yield 2 ^b [%]	Yield 3 ^b [%]
1	A (1)	1	Toluene	20	3	3	0
2	A (1)	1	THF	20	17	17	0
3	B (1)	0	Toluene	16	8	8	0
4	B (1)	0	THF	16	0	0	0
5	B (1)	0	Heptane	16	24	24	0
6 ^c	B (5)	0	Heptane	1	30	30	0
7 ^c	B (5)	0	Heptane	9	90	88	2
8 ^c	B (5)	0	—	9	70	69	1
9 ^c	C (5)	5	Heptane	2	45	44	1
10 ^c	C (5)	5	Heptane	16	98	88	10
11 ^c	C (5)	5	—	2	52	51	1
12 ^c	C (5)	5	—	16	92	90	2
13 ^c	D (5)	5	Toluene	2	100	93	7
14 ^c	E (5)	5	Cyclohexane	2, 6	27, 43	24, 39	3, 4
15 ^c	E (5)	5	Heptane	2, 6	17, 22	15, 18	2, 4
16 ^c	E (0.5)	0.5	— ^d	2, 6	1, 1	1, 1	0, 0
17 ^c	F (5)	5	Cyclohexane	2, 6	1, 7	0, 3	0, 4
18 ^c	F (5)	5	Heptane	2, 6	3, 9	2, 3	1, 6
19 ^c	F (0.5)	0.5	— ^d	2, 6	22, 27	18, 21	4, 6

^a 1.0 mmol of substrate. ^b Determined by GC with dodecane as internal standard. ^c Reaction temperature is 120 °C. ^d 10.0 mmol of substrate.

Table 2 Solvent and catalyst loading screening in the isomerization of oct-1-en-3-ol to 3-octanone^a


Entry	Cat. (%)	^t BuOK (%)	Solvent	Time (h)	Conv. ^b [%]	Yield 2 ^b [%]	Yield 3 ^b [%]
1	5	5	Toluene	2	100	93	4
2	5	5	1,4-Dioxane	2	100	98	1
3	5	5	Cyclohexane	2	100	93	7
4	5	5	Heptane	2	100	87	10
5	5	5	No	2	100	97	3
6	1	1	1,4-Dioxane	1	100	100	0
7 ^c	1	1	1,4-Dioxane	1, 16	88, 100	76, 83	10, 15
8 ^d	0.1	0.1	1,4-Dioxane	1	70	68	2
9 ^d	0.1	0.1	Cyclohexane	1	97	95	2
10 ^d	0.1	0.1	Toluene	1	100	99	1
11 ^e	0.1	0.1	Toluene	1	85	85	0
12 ^f	0.1	0.1	No	1	94	94	0
13 ^c	0.1	0.1	No	16	6	6	0
14 ^g	0.01	0.01	No	16	3	3	0

^a 1.0 mmol of substrate. ^b Determined by GC with dodecane as internal standard. ^c Room temperature. ^d 10.0 mmol of substrate and 10 mL of solvent. ^e 10.0 mmol of substrate and 10 mL of solvent, open system. ^f 10.0 mmol of substrate. ^g 100.0 mmol of substrate.

reduced the catalyst loading to 0.01 mol% while increasing at the same time the amount of substrate (100 mmol) (entry 14). The latter resulted in a turnover number (TON) of 300 and was obtained in the absence of any solvent. Nevertheless, the use of solvent is still preferred due to the slightly higher turnover frequency (TOF) which can be achieved (1000 h⁻¹, entry 10) compared to the neat conditions (TOF: 940 h⁻¹, entry 12).

2.2 Substrate scope

With the optimized reaction conditions in hand, we subsequently tested the scope and limitations of this catalytic system which included various aromatic and aliphatic allylic alcohols (Table 3). Excellent yields of the ketones were obtained in the isomerization of aromatic allylic alcohols and homo-allylic alcohols. Both electron-rich and electron-poor substituents on the aromatic ring were well-tolerated (entries 1–11). Isomerization of 1-phenylprop-2-en-1-ol which was selected as the parent substrate resulted in a 91% yield of the corresponding ketone (entry 1). A methyl substituent on the *para*-position of the aromatic ring had no influence on the yield of the desired product (entry 2). A slight decrease of the catalytic activity was observed when the methyl substituent was replaced by a methoxy group in the *para* position of the aromatic ring (entry 3). A bromo-substituent was also well-tolerated and isomerization of the *para*-bromo compound led to formation of the ketone in 87% yield (entry 4). An excellent yield (89%) was obtained when the reaction was carried out on the naphthyl derivative (entry 5). Substrates with heteroaromatic rings, *e.g.* furanyl- and thienyl-, showed high isomerization activity in terms of the yield of the desired ketones (entries 6 and 7). The substrate with an internal double bond was also converted into the corresponding

carbonyl compound in 95% yield (entry 8). Interestingly, good to excellent yields of the corresponding carbonyl derivatives were also obtained by using homo-allylic alcohols (entries 9–11) which have a carbon number of exact one between the alcohol and the double bond functionality. In comparison, when the carbon number is equal to two (entry 12), no isomerization reaction took place, which nicely confirms that the isomerisation does not take place *via* a metal-catalysed double bond isomerization. In the case of the homo-allylic alcohols we assume that the double bond is shifted by base catalysis at the unsaturated ketone stage. Aliphatic allylic alcohols could also be converted to the ketones in good yield. 1-Cyclohexyl-but-2-en-1-ol (entry 13), which was used as a mixture of *cis*- and *trans*-isomers, was converted to 1-cyclohexylbutan-1-one in a high isolated yield. Linear allylic alcohols were isomerized to the saturated ketones with excellent yields using this catalytic system (entry 14 and 15). Notably, when we used 10 mmol (1.5 gram scale) of oct-1-en-3-ol as substrate in 10 mL of toluene, the purification procedure of 3-octanone required only filtering off the catalyst and salts and removal of the solvent.

2.3 Mechanism – theory and experiment

We also carried out a computational study to understand the kinetic and thermodynamic parameters of the reaction. All computational details are given in the ESI.†

Both previous experimental and computational studies showed that the bromo-amine complex [Mn(Br)(CO)₂HN(CH₂CH₂PR₂)] (Fig. 1, A and D) is the pre-catalyst and needs to be activated by base to form the amido catalyst [Mn(CO)₂N(CH₂CH₂PR₂)]. Isomerization from 1 to 2 *via* the proposed outer-sphere mechanism in Scheme 1 was computed. According to the proposed mechanism, the first

Table 3 Substrate scope of manganese-catalyzed allylic/homo-allylic alcohol isomerization^a

$\text{R}^2\text{-(CH}_2\text{)}_n\text{-CH(OH)-CH=CH-R}^1 \xrightarrow[\text{Toluene, 120 }^\circ\text{C, 1 h}]{1 \text{ mol\% cat. D} + 1 \text{ mol\% } t\text{BuOK}}$ $\text{R}^2\text{-(CH}_2\text{)}_n\text{-C(=O)-CH}_2\text{-CH}_2\text{-R}^1$ $n=1, 0$			
Entry	Allylic/homo-allylic alcohols	Ketones	Yield ^b
1			91
2			90
3			74
4			87
5			89
6			91
7			96
8			95
9			93
10			93
11			73
12			0
13			93
14			94
15			91

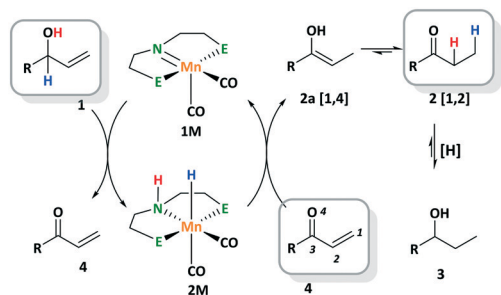
^a 1.0 mmol of substrate, 1 mol% of catalyst **D**, 1 mol% of *t*BuOK, 1 mol of toluene. ^b Isolated yield.

step is the dehydrogenation of allyl alcohol **1** to α,β -unsaturated ketone **4** by using complex **1M-iPr/Ph**.

In our previous study of the ketone hydrogenation by using **2M**,¹⁶ which is the reverse reaction of the dehydrogenation reaction, we found a two-step process, in which the first step is the hydride transfer from M-H to the

carbon center of ketone, followed by an ion-pair intermediate and the second step is the proton transfer from N-H to the oxygen center of ketone; and the hydride transfer is the rate-determining step.

On the basis of these results, we also tried to locate a revised two-step process for the dehydrogenation reaction.



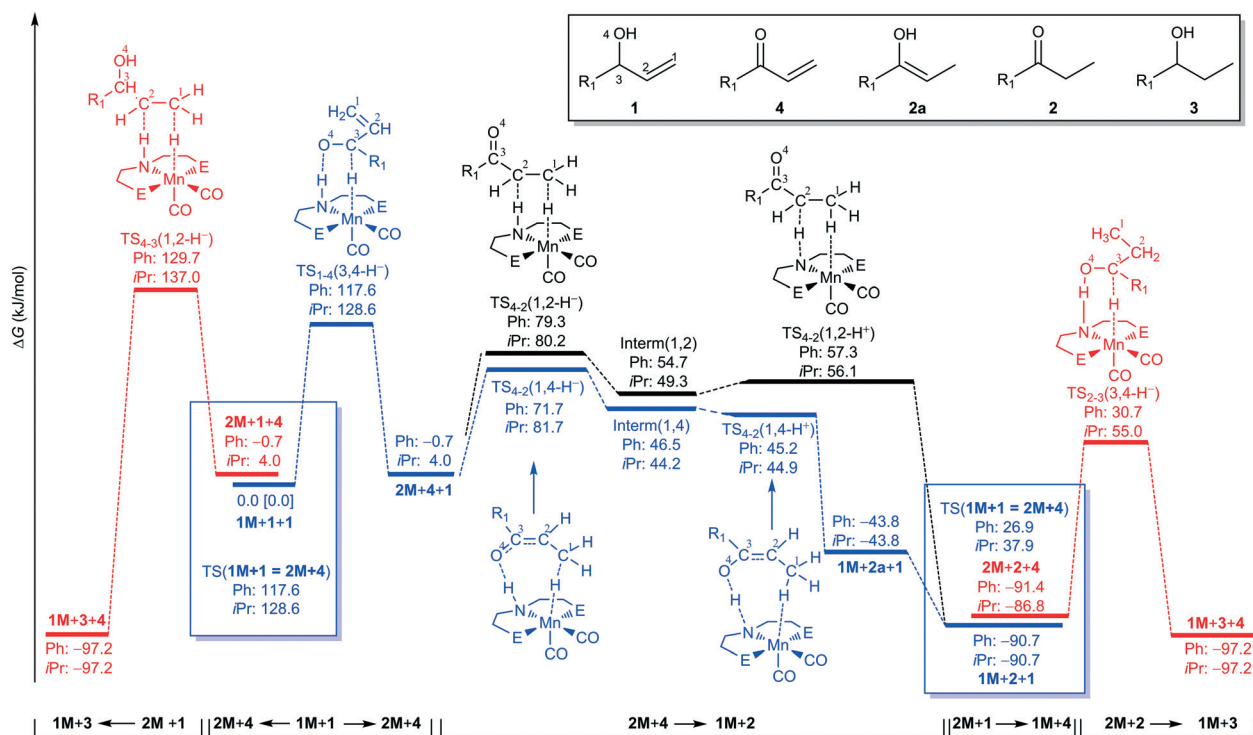
Scheme 1 Proposed mechanism ($R = C_5H_{11}$, $E = P(iPr)_2$ or PPh_2).

However, only one transition state corresponding to the hydride transfer [$TS_{1-4}(3,4-H^-)$] was located for the dehydrogenation of allyl alcohol 1; and neither the expected transition state of the proton transfer nor the ion-pair intermediate could be located. It shows that the dehydrogenation of allyl alcohol 1 follows a concerted mechanism. Actually, similar results have been found for the reaction catalyzed by using the corresponding Fe-PNP¹² as well as Ru-PNP¹⁷ complexes. It is found that the hydride transfer has a Gibbs free energy barrier of 128.6 and 117.6 kJ mol^{-1} for **1M-iPr** and **1M-Ph**, respectively; and the reaction is endergonic by 4.0 kJ mol^{-1} for **1M-iPr** and somewhat exergonic by 0.7 kJ mol^{-1} for **1M-Ph**; indicating a quite thermodynamically balanced process.

The next step is the C=C bond hydrogenation of the α,β -unsaturated ketone 4 by using complex **2M-iPr/Ph** via either 1,2-addition directly to 2 or via 1,4-addition to form the enol

2a, which can tautomerize into 2. For the 1,2-addition, we found a stepwise mechanism; *i.e.*; the first step is the hydride transfer of Mn-H to the terminal C¹ carbon via the transfer state $TS_{4-2}(1,2-H^-)$ resulting in the formation of the ion-pair intermediate **interm(1,2)**. The second step is the proton transfer of N-H to the internal C² carbon via the transition state of $TS_{4-2}(1,2-H^+)$. The free energy barrier of the first step is 76.2 and 80.0 kJ mol^{-1} for **2M-iPr** and **2M-Ph**, respectively. The formation of **interm(1,2)** is endergonic by 45.3 and 55.4 kJ mol^{-1} for **2M-iPr** and **2M-Ph**, respectively.

The second step has free energy barrier of 52.1 and 58.0 kJ mol^{-1} for **2M-iPr** and **2M-Ph**, respectively. Totally, the first step is rate-determining; and this hydrogenation is exergonic by 94.7 and 90.0 kJ mol^{-1} for **2M-iPr** and **2M-Ph**, respectively. For the 1,4-addition, we also found a stepwise mechanism; *i.e.*; the first step is the hydride transfer of Mn-H to the terminal C¹ carbon via the transfer state $TS_{4-2}(1,4-H^-)$ resulting in the formation of the ion-pair intermediate **interm(1,4)**. The second step is the proton transfer of N-H to the terminal O⁴ via the transition state of $TS_{4-2}(1,4-H^+)$. The free energy barrier of the first step is 77.7 and 72.4 kJ mol^{-1} for **2M-iPr** and **2M-Ph**, respectively. The formation of **interm(1,4)** is endergonic by 40.2 and 47.2 kJ mol^{-1} for **2M-iPr** and **2M-Ph**, respectively. The second step has a free energy barrier of 40.9 and 45.9 kJ mol^{-1} for **2M-iPr** and **2M-Ph**, respectively. The tautomerization from **2a** to 2 is exergonic by 46.9 kJ mol^{-1} . The first step is rate-determining. Comparison in Scheme 2 shows that the 1,4-route is more favored kinetically than the 1,2-route for **2M-Ph** (80.0 vs. 72.4



Scheme 2 Gibbs free energy profile for the isomerization of 1 to 2 ($R_1 = C_5H_{11}$, $E = P(iPr)_2$ or $P(Ph)_2$).

kJ mol^{-1}) by 7.6 kJ mol^{-1} , whereas the 1,4- and 1,2-routes have close barriers (77.7 and 76.2 kJ mol^{-1} , respectively) for **2M-iPr**.

Compared with the dehydrogenation of **1** to **4**, the hydrogenation of **4** to **2** is more favored kinetically by 52.4 ($128.6 \text{ kJ mol}^{-1}$ for **1M-iPr** vs. 76.2 kJ mol^{-1} for **2M-iPr**) and 45.2 kJ mol^{-1} ($117.6 \text{ kJ mol}^{-1}$ for **1M-Ph** vs. 72.4 kJ mol^{-1} for **2M-Ph**), and thermodynamically by 94.7 (-90.7 vs. 4.0 kJ mol^{-1}) and 90.0 kJ mol^{-1} (-90.7 vs. -0.7 kJ mol^{-1}) for **1M-iPr** and **1M-Ph**. Therefore, once **4** formed, it can be easily converted to **2**. The detailed course of the dehydrogenation step of alcohols by a manganese PNP pincer complex was previously described by Gauvin and coworkers.^{6b} In agreement with their findings, an immediate color change (red to yellow) was noticed when an allylic alcohol was added. This observation is associated to the formation of an alkoxide species which, when heated further becomes the amino hydride species **2M**.

In addition, we computed the direct hydrogenation of **1** to **3** by using complexes **2M-iPr/Ph** after the dehydrogenation of one equivalent **1** into **4**. For **1** hydrogenation to **3**, this reaction proceeds *via* a one-step mechanism mainly corresponding to the hydride transfer and is exergonic by 101.2 and 96.5 kJ mol^{-1} for **2M-iPr** and **2M-Ph**, respectively. The barrier is 133.0 and $133.4 \text{ kJ mol}^{-1}$ for **2M-iPr** and **2M-Ph**, respectively. This indicates that the isolated C=C double bond hydrogenation of **1** is less competitive kinetically than the conjugated C=C double bond hydrogenation of **4** by 56.8 (133.0 vs. 76.2 kJ mol^{-1}) for **2M-iPr** and 61.0 kJ mol^{-1} (133.4 vs. 72.4 kJ mol^{-1}) for **2M-Ph**.

Furthermore, we computed the consecutive hydrogenation of **2** to **3** by using complexes **2M-iPr/Ph** after the dehydrogenation of another one equivalent **1** into **4**. The hydrogenation of **2** to **3** by using complex **2M-iPr/Ph** is found to have a one-step process. The computed barrier is 141.8 and $122.1 \text{ kJ mol}^{-1}$ for **2M-iPr** and **2M-Ph**, respectively; and the reaction is exergonic by 10.4 and 5.8 kJ mol^{-1} for **2M-iPr** and **2M-Ph**, respectively.

All these reveal that **2** is the principal and preferred product. The hydrogenation of the isolated C=C bond from **1** to **3** and the isolated C=O bond from **2** to **3** by using complex **2M-iPr/Ph** are not competitive kinetically. This agrees perfectly with the results that the ketone is the major product.

To investigate the stability of the catalysts (Fig. 2), we computed the dehydrogenation or hydrogen elimination from complex **2M-iPr/Ph** to complex **1M-iPr/Ph** ($2\text{M} = 1\text{M} + \text{H}_2$), which has a Gibbs free energy barrier of 89.5 and 86.4 kJ mol^{-1} for **2M-iPr** and **2M-Ph**, respectively; is slightly exergonic by 1.3 kJ mol^{-1} for **2M-iPr**, while slightly endergonic by 3.3 kJ mol^{-1} for **2M-Ph**.

Comparisons show that the barrier of H_2 elimination from **2M-iPr/Ph** to complex **1M-iPr/Ph** is higher than that of the hydrogenation of **4** to **2** and lower than that of the dehydrogenation of **1** to **4**. This reveals that the dehydrogenation of **1** to **4** is the rate-determining step on the

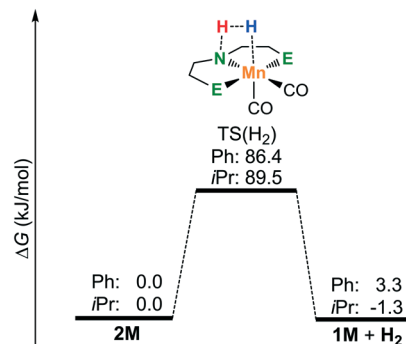


Fig. 2 Gibbs free energy profile of H_2 elimination from **2M**. (E = $\text{P}(\text{iPr})_2$ or $\text{P}(\text{Ph})_2$).

whole potential energy surface. Since the barrier of H_2 elimination is lower than that of **1** to **4** dehydrogenation, it is necessary to run the reaction in a closed system in order to maintain the stability of the catalyst **2M-iPr/Ph**. This explains clearly why the reaction needs to be carried out in a pressure tube. Nevertheless, when the reaction on **1** was performed in an open system, only a slightly lower yield (87%) of **2** was obtained (Table 2, entry 11).

It is noted that the free energy barrier of **1M-Ph** is lower than **1M-iPr** by 11.0 kJ mol^{-1} in the process from **1** to **4**, and by 10.0 kJ mol^{-1} in the 1,4-route from **4** to **2**. This shows the more favored substitution effect of phenyl over isopropyl. Therefore, we employed the proposed activation strain model¹⁸ (ASM, Fig. 2) to investigate the substitution effect. According to the ASM scheme, we dissected the electronic activation energy of the transition states of rate-determining step ($\text{TS}_{1-4}(3,4\text{-H}^-)$, ΔE^\ddagger) into the geometrical strain energy (ΔE_{strain}) and interaction energy (ΔE_{int}), where the electronic activation energy ΔE^\ddagger is the electronic energy difference between the optimized TS and the sum of substrate and catalyst in their optimized structures; and the geometrical strain energy $\Delta E_{\text{strain}}^\ddagger$ is the electronic energy difference between the sum of the structurally deformed substrate and catalyst individually taken from the optimized TS and the sum of reactant and catalyst in their optimized structures. Accordingly, the difference between $\Delta E_{\text{strain}}^\ddagger$ and ΔE^\ddagger is the interaction energy between substrate and catalyst in the TS. In addition, $\Delta E_{\text{strain}}^\ddagger$ can be divided into

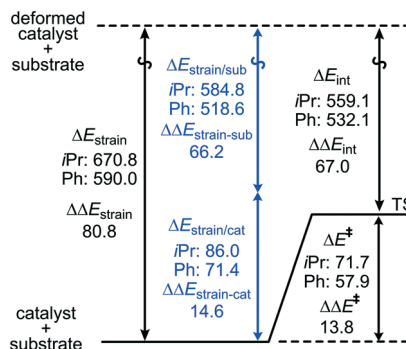
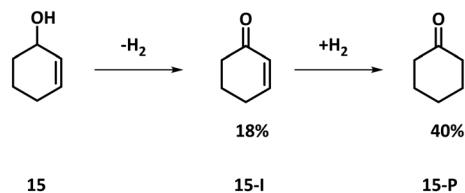


Fig. 3 ASM analysis of $\text{TS}_{1-4}(3,4\text{-H}^-)$ of reaction $[1\text{M} + 1 = 2\text{M} + 4]$.



Scheme 3 Slow isomerization of cyclohexenol allows isolation of the intermediate **15-I**. Conditions: 2.0 mmol, 1 mol% **D**, 1 mol% ^tBuOK, 2 mL toluene, 120 °C, 3 h.

the strain energy of substrate ($\Delta E_{\text{strain/sub}}^{\ddagger}$) and catalyst ($\Delta E_{\text{strain/cat}}^{\ddagger}$) accordingly ($\Delta E_{\text{strain}}^{\ddagger} = \Delta E_{\text{strain/sub}}^{\ddagger} + \Delta E_{\text{strain/cat}}^{\ddagger}$). All these data based on reactions [**1M** + **1** = **2M** + **4**] are shown in Fig. 3.

As shown in Fig. 3, for the hydrogenation of **1** to **4**, the energy barrier of **TS**₁₋₄(**3,4-H**)–**Ph** is lower in energy than that of the **TS**₁₋₄(**3,4-H**)–**iPr** ($\Delta\Delta E^{\ddagger} = \Delta E^{\ddagger}(\text{iPr}) - \Delta E^{\ddagger}(\text{Ph})$) by 13.8 kJ mol⁻¹. Further analyses into the difference of geometrical strain energy ($\Delta\Delta E_{\text{strain}}^{\ddagger} = \Delta E_{\text{strain}}^{\ddagger}(\text{iPr}) - \Delta E_{\text{strain}}^{\ddagger}(\text{Ph})$) and interaction energy ($\Delta\Delta E_{\text{int}}^{\ddagger} = \Delta E_{\text{int}}^{\ddagger}(\text{iPr}) - \Delta E_{\text{int}}^{\ddagger}(\text{Ph})$) reveal that the $\Delta\Delta E^{\ddagger}$ is dominated by $\Delta\Delta E_{\text{strain}}^{\ddagger}$. In addition, the $\Delta\Delta E_{\text{strain/sub}}^{\ddagger}$ contributes much stronger than the $\Delta\Delta E_{\text{strain/cat}}^{\ddagger}$.

These results revealed that the isopropyl substituted Mn PNP catalyst causes larger structural distortion for the substrate in the transition state than phenyl substituted Mn PNP catalyst, and explains why the phenyl substituted catalysts (**1M/2M-Ph**) shows higher activity than the isopropyl substituted catalysts (**1M/2M-iPr**).

These computational results highlight a consecutive dehydrogenation–hydrogenation sequence. According to this, cyclohexenol (**15**) was chosen as a substrate in order to find cyclohexenone (**15-I**) as an intermediate which requires typically more time for alkene hydrogenation in comparison to the before mentioned substrates.¹² Hence, after 3 h at 120 °C (Scheme 3) a mixture of starting material (**15**), the intermediate (**15-I**) and the desired product cyclohexanone (**15-P**) was obtained. The overall conversion of cyclohexenol is quite low (58%) whereby 18% were found to be the intermediate **15-I**. This discovery not only supports the evidence of a dehydrogenation–hydrogenation mechanism but also the fact that the dehydrogenation is the rate-determining step.

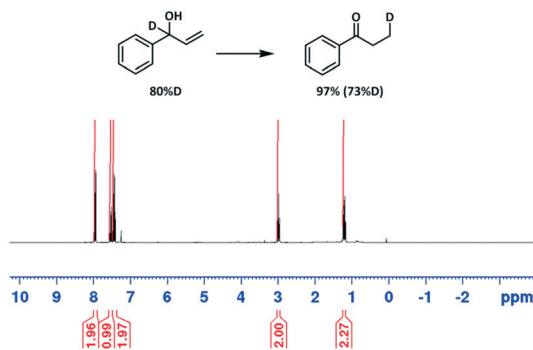


Fig. 4 Deuterium labeling experiment. Conditions: 1.0 mmol, 1 mol% **D**, 1 mol% ^tBuOK, 1 mL toluene, 120 °C, 1 h.

To supply further proof for the proposed mechanism we have performed a deuterium labeling experiment. Applying the same conditions as used for the substrate scope, 1-D-labelled 1-phenylprop-2-en-1-ol (Fig. 4) was isomerized efficiently to the corresponding ketone. From this reaction the saturated ketone was recovered exclusively labeled in the beta-position. This result is in perfect agreement with our proposed dehydrogenation-1,4- reduction pathway.

3. Conclusions

In summary, we have shown for the first time that manganese complexes are efficient catalysts for the isomerization of allylic alcohols to the corresponding ketones with catalyst amounts as low as 0.1 mol% in the presence of base. Notably, the efficiency of the catalysts could be increased by changing the substituent on the phosphorus atom from isopropyl to phenyl. Good to excellent yields could be achieved in both aromatic and aliphatic allylic or homo-allylic alcohols. A two-step self-hydrogen borrowing mechanism involving dehydrogenation–hydrogenation isomerization is proposed and verified by DFT computations. The calculated results in verifying the selectivity and revealing the higher activity of the phenyl over isopropyl substitution are in perfect agreement with experiments. The high activity of phenyl over isopropyl substitution is due to the weaker structural strain of the substrate interacting with the phenyl substitution than isopropyl substitution, and this is responsible for the lower barrier for phenyl substitution.

Experimental section

Synthesis of catalyst **D**

A suspension of HCl-PNP^(Ph) ligand (600 mg, 1.26 mmol) and NEt₃ (0.2 mL, 1.45 mmol) in THF (20 mL) was stirred for 15 minutes at room temperature. The liquid part of the resulting suspension was added dropwise through cannula filtration to a suspension of Mn(CO)₅Br (275 mg, 1.0 mmol) in THF (40 mL) (be aware of CO evolution). After one hour, the mixture was heated to 100 °C and stirred for 24 hours (a precipitate was formed during the course of the reaction). After this time, the mixture was allowed to cool to room temperature and the suspension was filtered. The resulting solid was washed with heptane (3 × 20 mL) and dried *in vacuo* to afford the title compound (388 mg, 61%). Single crystals suitable for X-ray diffraction measurement were obtained from slow diffusion of heptane into the solution of the title compound in toluene.

General procedure for the isomerization of allylic alcohols

An oven dried 10 mL pressure tube with a stirring bar was charged with complex **D** (0.01 mmol, 1 mol%), 0.01 mmol ^t-BuOK and 1 mL toluene sequentially. Then 1 mmol of substrate was added immediately to the pressure tube. The solution was stirred for 1 hour at 120 °C. GC yields were determined with *n*-dodecane as internal standard. Isolated yields were obtained by using silica gel chromatography

(cyclohexane : ethyl acetate = 50 : 1) after rotary evaporation. For the neat reaction, base was added together with complex D.

Conflicts of interest

The authors declare that there is no conflict of interest.

Acknowledgements

Tian Xia is grateful for the financial support of Chinese Scholarship Council (CSC). This work was also supported by the state of Mecklenburg-Vorpommern and the Leibniz Association (Leibniz Competition, SAW-2016-LIKAT-1523). We are also thankful to Marcel Garbe (Leibniz-Institute for Catalysis) for the provision of some chemicals.

Notes and references

- 1 B. M. Trost, *Angew. Chem., Int. Ed. Engl.*, 1995, **34**, 259.
- 2 (a) M. Hassam, A. Taher, G. E. Arnott, I. R. Green and W. A. van Otterlo, *Chem. Rev.*, 2015, **115**, 5462; (b) A. Vasseur, J. Bruffaerts and I. Marek, *Nat. Chem.*, 2016, **8**, 209.
- 3 (a) R. C. van der Drift, E. Bouwman and E. Drent, *J. Organomet. Chem.*, 2002, **650**, 1; (b) R. Uma, C. Crévisy and R. Grée, *Chem. Rev.*, 2003, **103**, 27; (c) V. Cadierno, P. Crochet and J. Gimeno, *Synlett*, 2008, 1105; (d) L. Mantilli and C. Mazet, *Chem. Lett.*, 2011, **40**, 341; (e) N. Ahlsten, A. Bartoszewicz and B. Martín-Matute, *Dalton Trans.*, 2012, **41**, 1660; (f) P. Lorenzo-Luis, A. Romerosa and M. Serrano-Ruiz, *ACS Catal.*, 2012, **2**, 1079; (g) D. Cahard, S. Gaillard and J.-L. Renaud, *Tetrahedron Lett.*, 2015, **56**, 6159; (h) H. Li and C. Mazet, *Acc. Chem. Res.*, 2016, **49**, 1232.
- 4 (a) H.-X. Zheng, Z.-F. Xiao, C.-Z. Yao, Q.-Q. Li, X.-S. Ning, Y.-B. Kang and Y. Tang, *Org. Lett.*, 2015, **17**, 6102; (b) S. Martinez-Erro, A. Sanz-Marco, A. Bermejo Gómez, A. Vázquez-Romero, M. S. G. Ahlquist and B. Martín-Matute, *J. Am. Chem. Soc.*, 2016, **138**, 13408; (c) H.-X. Zheng, C.-Z. Yao, J.-P. Qu and Y.-B. Kang, *Org. Chem. Front.*, 2018, **5**, 1213.
- 5 (a) S. Elangovan, C. Topf, S. Fischer, H. J. Jiao, A. Spannenberg, W. Baumann, R. Ludwig, K. Junge and M. Beller, *J. Am. Chem. Soc.*, 2016, **138**, 8809; (b) F. Kallmeier, T. Irrgang, T. Dietel and R. Kempe, *Angew. Chem., Int. Ed.*, 2016, **55**, 11806; (c) A. Bruneau-Voisine, D. Wang, T. Roisnel, C. Darcel and J. B. Sortais, *Catal. Commun.*, 2017, **92**, 1; (d) N. A. Espinosa-Jalapa, A. Nerush, L. J. W. Shimon, G. Leitius, L. Avram, Y. Ben-David and D. Milstein, *Chem. – Eur. J.*, 2017, **23**, 5934; (e) M. Garbe, K. Junge, S. Walker, Z. H. Wei, H. J. Jiao, A. Spannenberg, S. Bachmann, M. Scalone and M. Beller, *Angew. Chem., Int. Ed.*, 2017, **56**, 11237; (f) H. Y. Ge, X. Y. Chen and X. Z. Yang, *Chem. – Eur. J.*, 2017, **23**, 8850; (g) K. S. Rawat and B. Pathak, *Catal. Sci. Technol.*, 2017, **7**, 3234; (h) M. Glatz, B. Stöger, D. Himmelbauer, L. F. Veiros and K. Kirchner, *ACS Catal.*, 2018, **8**, 4009.
- 6 (a) R. He, Z.-T. Huang, Q.-Y. Zheng and C. Wang, *Angew. Chem., Int. Ed.*, 2014, **53**, 4950; (b) D. H. Nguyen, X. Trivelli, F. Capet, J.-F. Paul, F. Dumeignil and R. M. Gauvin, *ACS Catal.*, 2017, **7**, 2022; (c) M. Andérez-Fernández, L. K. Vogt, S. Fischer, W. Zhou, H. J. Jiao, M. Garbe, S. Elangovan, K. Junge, H. Junge, R. Ludwig and M. Beller, *Angew. Chem., Int. Ed.*, 2017, **56**, 559.
- 7 (a) A. Bruneau-Voisine, D. Wang, V. Dorcet, T. Roisnel, C. Darcel and J. B. Sortais, *Org. Lett.*, 2017, **19**, 3656; (b) M. Perez, S. Elangovan, A. Spannenberg, K. Junge and M. Beller, *ChemSusChem*, 2017, **10**, 83; (c) A. Zirakzadeh, S. de Aguiar, B. Stoger, M. Widhalm and K. Kirchner, *ChemCatChem*, 2017, **9**, 1744; (d) K. Z. Demmans, M. E. Olson and R. H. Morris, *Organometallics*, 2018, **37**, 4608; (e) O. Martínez-Ferraté, C. Werlé, G. Francio and W. Leitner, *ChemCatChem*, 2018, **10**, 4514; (f) D. Wang, A. Bruneau-Voisine and J. B. Sortais, *Catal. Commun.*, 2018, **105**, 31.
- 8 (a) A. Brzozowska, L. M. Azofra, V. Zubar, I. Atodiresei, L. Cavallo, M. Rueping and O. El-Sepelgy, *ACS Catal.*, 2018, **8**, 4103; (b) Y. P. Zhou, Z. B. Mo, M. P. Luecke and M. Driess, *Chem. – Eur. J.*, 2018, **24**, 4780.
- 9 (a) W. Liu and L. Ackermann, *ACS Catal.*, 2016, **6**, 3743; (b) Y. Hu, B. Zhou and C. Wang, *Acc. Chem. Res.*, 2018, **51**, 816.
- 10 X. Yang and C. Wang, *Chem. – Asian J.*, 2018, **13**, 2307.
- 11 (a) S. Elangovan, J. Neumann, J. B. Sortais, K. Junge, C. Darcel and M. Beller, *Nat. Commun.*, 2016, **7**, 12641; (b) M. Peña-López, P. Piehl, S. Elangovan, H. Neumann and M. Beller, *Angew. Chem., Int. Ed.*, 2016, **55**, 14967; (c) M. K. Barman, A. Jana and B. Maji, *Adv. Synth. Catal.*, 2018, **360**, 3233; (d) S. Chakraborty, P. Daw, Y. Ben David and D. Milstein, *ACS Catal.*, 2018, **8**, 10300; (e) A. Jana, C. B. Reddy and B. Maji, *ACS Catal.*, 2018, **8**, 9226; (f) Y. K. Jang, T. Krückel, M. Rueping and O. El-Sepelgy, *Org. Lett.*, 2018, **20**, 7779; (g) V. G. Landge, A. Mondal, V. Kumar, A. Nandakumar and E. Balaraman, *Org. Biomol. Chem.*, 2018, **16**, 8175; (h) T. T. Liu, L. D. Wang, K. K. Wu and Z. K. Yu, *ACS Catal.*, 2018, **8**, 7201; (i) G. Y. Zhang, T. Irrgang, T. Dietel, F. Kallmeier and R. Kempe, *Angew. Chem., Int. Ed.*, 2018, **57**, 9131; (j) J. C. Borghs, Y. Lebedev, M. Rueping and O. El-Sepelgy, *Org. Lett.*, 2019, **21**, 70.
- 12 (a) T. Xia, Z. Wei, B. Spiegelberg, H. Jiao, S. Hinze and J. G. de Vries, *Chem. – Eur. J.*, 2018, **24**, 4043; (b) B. Spiegelberg, A. Dell'Acqua, T. Xia, A. Spannenberg, S. Tin, S. Hinze and J. G. de Vries, *Chem. – Eur. J.*, 2019, **25**, 7820.
- 13 A. T. Radosevich, J. G. Melnick, S. A. Stoian, D. Bacciu, C.-H. Chen, B. M. Foxman, O. V. Ozerov and D. G. Nocera, *Inorg. Chem.*, 2009, **48**, 9214.
- 14 A. M. Tondreau and J. M. Boncella, *Polyhedron*, 2016, **116**, 96.
- 15 A. Mukherjee, A. Nerush, G. Leitius, L. J. W. Shimon, Y. Ben David, N. A. E. Jalapa and D. Milstein, *J. Am. Chem. Soc.*, 2016, **138**, 4298.
- 16 S. Elangovan, C. Topf, S. Fischer, H. Jiao, A. Spannenberg, W. Baumann, R. Ludwig, K. Junge and M. Beller, *J. Am. Chem. Soc.*, 2016, **138**, 8809.
- 17 R. A. Farrar-Tobar, Z. Wei, H. Jiao, S. Hinze and J. G. de Vries, *Chem. – Eur. J.*, 2018, **24**, 2725.
- 18 I. Fernández and F. M. Bickelhaupt, *Chem. Soc. Rev.*, 2014, **43**, 4953.